NJC

PAPER

Oxadiazole containing poly(*p*-phenylenevinylene)s: synthesis and characterization†

Pengfei Li,‡ Shanpeng Wen,‡ Weidong Cheng, Jibo Zhang, Shiyu Yao, Bin Xu and Wenjing Tian*

A series of poly(*p*-phenylenevinylene) based polymers (MEH-OXD-PPVs) functionalized with Y-shaped double 1,3,4-oxadiazole-containing side chains were synthesized through a modified Gilch reaction. They are all soluble in common organic solvents such as chloroform, tetrahydronfuran and 1,1,2,2-tetrachloroethane. The chemical structures of MEH-OXD-PPVs were determined by ^{1}H NMR, GPC and elemental analysis. Thermogravimetric analysis shows that they have good thermal stability with the decomposition temperature ranging from 312 °C to 326 °C. The absorption and fluorescence emission maxima of the polymers exhibit an appreciable blue-shift with the increase of oxadiazole-containing moieties. Electrochemical investigation shows that the HOMO energy levels of the polymers vary regularly with the change of content of oxadiazole-containing moieties. Additionally, by introducing more OXD-PV unit during copolymerization, the PL quantum efficiencies of the polymers are significantly enhanced compared to that of MEH-PPV. The successful manipulation of optical and electronic properties of the MEH-OXD-PPVs indicates an effective concept for developing PPV-based functional materials with tunable optoelectronic properties by changing the amount of electron-withdrawing oxadiazole-containing moieties.

Introduction

Conjugated polymers have excellent optoelectronic properties which are currently being employed in various applications, such as light-emitting diodes (LEDs), photovoltaic cells (PVCs), thin film transistors (TFTs), and solid-state lasers[1–10] due to their feasible design of the molecular structures and easy modification of their photophysical properties.[11] Besides, conjugated polymers also provide many merits over inorganic materials such as low cost, easy processability, ease of forming large areas, and mechanical flexibility.[12]

Among various conjugated polymers, poly(*p*-phenylene vinylene) (PPV) and its derivatives have attracted tremendous attention due to their excellent luminescent and mechanical properties. Their ease of processing, long device lifetime as well as amenability to chemical modifications offer additional reasons for further investigation of this class of materials.[13] For example, by proper modification of the chemical structure, the fluorescence of PPVs can span over the visible range and further into the near-infrared region.

However, most of the PPVs have good hole-transport properties but poor electron-transport abilities with the hole mobility being about one to three orders of magnitude higher than the electron mobility,[14] which limits their applications as active materials in polymer LEDs and PVCs.[15–21] To overcome this drawback, one of the most widely employed methods is to enhance the electron affinity of the conjugated polymers by introducing electron-withdrawing groups, such as the 1,3,4-oxadiazole unit.[22]

The 1,3,4-oxadiazole unit is a very popular chromophore in organic small molecules and polymers for optoelectronic devices, notably for organic LEDs and PVCs.[12,23] The electron-deficient nature of oxadiazole can help to improve the electron mobility when incorporated into organic optoelectronic materials. In addition, the oxadiazole moiety is known to provide enhanced thermal stability, redox stability, and good film-forming properties.[24,25] Therefore, enormous efforts have been devoted to incorporate oxadiazole moieties into polymers either as polymer backbones[26–29] or as side chains[14,22–24] in order to develop new materials with improved optical and electronic properties. In comparison with main chain (backbone) modifications, side chain modifications have less impact on the hole-transport properties of the backbones; namely the main chain PPV does retain its own high hole mobility.[32] On the other hand, many efforts have been devoted to investigate the effect of oxadiazole concentration on the photophysical and electrochemical properties of polymers. Chen and co-workers once reported the influence of backbone-incorporated

State Key Laboratory of Supramolecular Structure and Materials, Jilin University, Changchun 130012, P. R. China. E-mail: wjtian@jlu.edu.cn; Fax: +86431 85193421; Tel: +86431 85166368

‡ These authors contributed equally to this work.

oxadiazole content on the photophysical and electrochemical properties of the resulting copolymers.[13] Being connected as part of the side chains, the content of the oxadiazole groups were also adjusted to tailor the chemical structures of the target copolymers to optimize their optical and electronic properties.[22,23] The above efforts have achieved some results in optimizing the polymer's photophysical properties, but they failed in tuning energy levels rationally; *i.e.*, they cannot simultaneously regulate photophysical and electrochemical properties by adjusting oxadiazole contents due to the linear pattern of used oxadiazole-containing side chains. Each linear side chain possesses only one oxadiazole unit, so it may not induce a sufficient electron-withdrawing ability that is strong enough to influence the energy levels of the polymer.

In this work, we present the synthesis of a series of new soluble PPV-based polymers with different mole ratios between two repeating units, {[2-(3-{3,5-bis[5-(4-dodecyloxy)phenyl]-1,3,4,-oxadiazole-2-yl}phenoxy)-hexyloxy-1,4-phenylenevinylene] (OXD-PV) and [2-methoxy-5-(2-ethylhexyloxy)-1,4-phenyl enevinylene] (MEH-PV). Instead of the commonly used linear side chain, a two-dimensional side chain is adopted in the target polymers. Being located at the end of flexible alkoxyl chain, phenyl ring possesses two branches in the *meta* positions. Each branch comprises three parts: a oxadiazole unit as the head, a phenylene spacer as the body, and a long flexible alkoxyl end chain as the tail. The whole two-dimensional side chain looks like a "Y", so it is named a Y-shaped side chain. The structural design is based on the consideration that the PPV backbone is a good hole-transporting material and the flexible alkoxyl chains provide solubility. Compared with the linear side chain that has one electron-deficient unit, each Y-shaped side chain contains two electron-deficient 1,3,4-oxadiazole units to provide a much enhanced electron-withdrawing ability. Through such a design, the Y-shaped side chain is expected to act more effectively in tuning the polymer's optical and electronic properties. Besides, the combination of branched alkoxyl chains with heterocyclic rings causes large steric hindrance, which would play an important role in influencing intermolecular interactions, thus in tailoring the photophysical properties of the target polymers. MEH-OXD-PPVs were synthesized by a modified Gilch polymerization method[12,23] and characterized by ^{1}H NMR, elemental analysis and GPC. Their photophysical and electrochemical properties were systematically described. As expected, the resulting polymers indeed exhibit good solubility in chloroform, tetrahydronfuran and 1,1,2,2-tetrachloroethane, as well as fine-tuned photophysical and electrochemical properties by adjusting the amount of the OXD-PV unit. Additionally, they possess high molecular weights (between 13 300 and 653 000) and good thermal stabilities. The successful regulation of optoelectronic properties of the MEH-OXD-PPVs leads to a clear understanding, at a molecular level, of the structure–property relationships in this series of materials.

Experimental section

Materials

N-Bromosuccinimide, 5-hydroxyisophthalate, potassium *tert*-butoxide (*t*-BuOK) were purchased from Acros. 1,3-Dibromo-propane, *p*-hydroxyanisole, POCl$_3$ and all the other solvents were purchased from Beijing Chemical Reagent. Tetrahydro-furan (THF) was dried over sodium and benzophenone. Diethyl 5-(3-bromopropoxy)-isophthalate, 1,4-bis(bromomethyl)-2-methoxy-5-(2-ethyl-hexy-loxy)benzene (monomer **7**) and poly(1-methoxy-4-(2-ethylhexyloxy)-*p*-phenylene vinylene) MEH-PPV were synthesized according to the literature.[12,30,31]

Measurements

^{1}H NMR spectra were recorded on Bruker AVANCE 500 MHz spectrometer with chloroform-d as solvent and tetramethylsilane (TMS) as internal standard. The elemental analysis was carried out with a Thermoquest CHNS-Ovelemental analyzer. The gel permeation chromatographic (GPC) analysis was carried out with a Waters 410 instrument with tetrahydrofuran as the eluent (flow rate: 1 mL min^{-1}, at 35 °C) and polystyrene as the standard. The thermogravimetric analysis (TGA) was performed on a Perkine Elmer Pyris 1 analyzer under nitrogen atmosphere (100 mL min^{-1}) at a heating rate of 10 °C min^{-1}. UV-visible absorption spectra were measured using a Shimadzu UV-3100 spectrophotometer. Photoluminescence spectra were collected on a Shimadzu RF-5301PC spectrophotometer and Maya 2000 Pro. optical fiber spectrophotometer. The PL quantum efficiencies were determined in an integrating sphere (C-701, Labsphere Inc.), with a 405 nm Ocean Optics LLS-LED as the excitation source, and the laser was introduced into the sphere through the optical fiber. Electrochemical measurements of these derivatives were performed with a Bioanalytical Systems BAS 100 B/W electrochemical workstation.

Synthesis of monomer

2-(6-Bromohexyloxy)-1,4-dimethylbenzene (1). 2,5-Dimethyl-phenol (6.10 g, 0.05 mol), 46 mL of 1,6-dibromo- hexane (0.30 mol), 30 g of anhydrous potassium carbonate, 0.3 g of KI, and 200 mL of dry acetone were refluxed for 24 h under N$_2$ atmosphere. The reaction mixture was cooled to room temperature, then it was filtered to remove the salts and concentrated under vacuum. The crude product was purified by column chromatography (hexane/ethyl acetate = 20 : 1) to give 11.16 g (90%) of a yellowy liquid. ^{1}H NMR (500 MHz, CDCl$_3$) (ppm, from TMS): 7.00(d, 1H), 6.66(d, 1H), 6.63(s, 1H), 3.95(t, 2H), 3.43(t, 2H), 2.31(s, 3H), 2.17(s, 3H), 1.90–1.89(m, 2H), 1.82–1.80(m, 2H), 1.54–1.52(m, 4H).

Diethyl 5-(6-(2,5-dimethylphenoxy)hexyloxy)isophthalate (2). Compound **1** (5.68 g, 0.02 mol), 4.76 g of diethyl 5-hydroxy-isophthalate (0.02 mol), 30 g of anhydrous potassium carbonate, 0.3 g of KI, and 200 mL of dry acetone were refluxed for 24 h under N$_2$ atmosphere. After being cooled to room temperature, the reaction mixture was filtered to remove the salts. The solvent was evaporated under vacuum and then the residue was poured into 200 mL of methanol under stirring. A white solid precipitated out, which was collected by filtration to give 7.15 g (80.8%) of compound **2**. ^{1}H NMR (500 MHz, CDCl$_3$) (ppm, from TMS): 8.27(s, 1H), 7.74(s, 2H), 7.00(d, 1H), 6.66–6.63(m, 2H), 4.42–4.37(m, 4H), 4.06(t, 2H), 3.96(t, 2H), 2.31(s, 3H), 2.17(s, 3H), 1.85–1.84(m, 4H), 1.60–1.57(m, 4H), 1.41(t, 6H). Anal. calcd for C$_{26}$H$_{34}$O$_6$: C, 70.56; H, 7.74. Found: C, 70.49; H, 7.79.

5-(6-(2,5-Dimethylphenoxy)hexyloxy)isophthalohydrazide (3).
Compound **2** (3.10 g, 0.007 mol), 30 mL (excess) of hydrazine monohydrate, and 60 mL of methanol were heated under reflux for 48 h. After being cooled to room temperature, the reaction mixture was recrystallized from ethanol. A white solid product was obtained with a total amount of 2.32 g (yield 80.1%). ^{1}H NMR (500 MHz, CDCl$_3$) (ppm, from TMS): 9.77(s, 2H), 7.85(s, 1H), 7.46(s, 2H), 6.98(d, 1H), 6.72(s, 1H), 6.62(d, 1H), 4.50(s, 4H), 4.06 (t, 2H), 3.95(t, 2H), 2.24(s, 3H), 2.08(s, 3H), 1.77–1.75(m, 4H), 1.51–1.49(m, 4H). Anal. calcd for C$_{22}$H$_{30}$N$_4$O$_4$: C, 63.75; H, 7.30; N, 13.52. Found: C, 63.70; H, 7.29; N, 13.45.

5,5′-(5-(6-(2,5-Dimethylphenoxy)hexyloxy)-1,3-phenylene)-bis(2-(4-(dodecyloxy)phenyl)-1,3,4-oxadiazole) (5). Compound **3** (2.90 g, 0.007 mol), 5 g (excess) of fresh 4-dodecyloxy-benzoyl chloride, 1.08 g of pyridine and 40 mL of THF were stirred at 0–5 °C for 4 h. The solvent was removed under reduced pressure to give a white sticky matter (compound **4**).

The obtained crude product was heated slowly for 30 min in 50 mL of POCl$_3$ under N$_2$ atmosphere. The mixture was refluxed for 8 h. After about 30 mL of POCl$_3$ was distilled off, the reaction mixture was cooled to room temperature and then poured into 300 mL of ice-water under stirring. After being extracted with chloroform (3 × 100 mL), the combined organic extracts were washed with water and NaHCO$_3$ (aq), dried over anhydrous MgSO$_4$. After removal of the solvent, the crude product was poured into a large amount of methanol. A yellow precipitate was collected by filtration and then it was recrystallized from methanol/chloroform. Two step yield 53%. ^{1}H NMR (500 MHz, CDCl$_3$) (ppm, from TMS): 8.40(s, 1H), 8.11(d, 4H), 7.81(s, 2H), 7.04(d, 4H), 7.00(d, 1H), 6.66–6.64(m, 2H), 4.17(t, 2H), 4.05(t, 4H), 3.98(t, 2H), 2.31(s, 3H), 2.18(s, 3H), 1.93–1.80(m, 10H), 1.63–1.61(m, 4H), 1.52–1.46(m, 4H), 1.38–1.27(m, 30H), 0.89(t, 6H). Anal. calcd for C$_{68}$H$_{82}$N$_4$O$_6$: C, 75.43; H, 8.65; N, 5.86. Found: C, 75.41; H, 8.70; N, 5.45.

1,3-Bis[2-(4-(dodecyloxy)phenyl)-1,3,4-oxidiazole-5-yl]-5-[3-(2,5-dibromomethyl)phenoxyhexyloxy]-benzene (6) (monomer 6). To a 250 mL three-neck flask, compound **5** (11.07 g, 11.6 mmol), *N*-bromosuccinimide (NBS) (4.6 g, 25.6 mmol), catalytic amounts of benzoyl peroxide (BPO), and 100 mL of benzene were added. The mixture was heated under reflux and stirred until succinimide was on top of the solution. After the disappearance of the compound **5**, confirmed by TLC, the mixture was cooled to room temperature. The succinimide was filtered off, and the mother liquor was poured into excess water. The mixture was extracted with dichloromethane, and the combined organic layers were washed several times further with water, dried over anhydrous MgSO$_4$. After filtration, the solvent was removed by evaporation under vacuum. The product was purified by column chromatography on silica gel using hexane to give 5.15 g (yield 40%) of Monomer 6. ^{1}H NMR (500 MHz, CDCl$_3$) (ppm, from TMS): 8.40(s, 1H), 8.11(d, 4H), 7.83(s, 2H), 7.281(s, 1H), 7.05 (d, 4H), 6.93–6.90(m, 2H), 4.54(s, 2H), 4.45(s, 2H), 4.19(t, 2H), 4.09(t, 2H), 4.05(t, 4H), 1.95–1.92(m, 4H), 1.86–1.80(m, 4H), 1.67–1.66(m, 6H), 1.52–1.46(m, 4H), 1.39–1.27(m, 34H), 0.89 (t, 6H). Anal. calcd for C$_{60}$H$_{80}$Br$_2$N$_4$O$_6$: C, 64.74; H, 7.24; Br, 14.36; N, 5.03. Found: C, 64.70; H, 7.29; Br, 14.31; N, 5.09.

Polymerization. All the polymerization reactions and manipulations were carried out under nitrogen atmosphere. The preparation of polymer **8a–8g** was conducted using the modified Gilch method.[12,23] The reaction conditions for the preparation of Polymer **8b–8g** were kept the same as that of polymer **8a**.

Polymer 8a (OXD-MEH-PPV(100/0)). A solution of 6 mL of potassium *tert*-butoxide (1.0 M THF solution, 6 mmol) was slowly added over 1 h to a stirred solution of monomer **6** (0.56 g, 0.5 mmol) in 25 mL of dry THF that was cooled to −5 °C. Under a N$_2$ atmosphere, the mixture was stirred at room temperature for 24 h. The polymerization solution was poured into 500 mL of MeOH. A crude polymer precipitated out, which was redissolved in chloroform and reprecipitated into methanol. Then the residue was extracted with methanol for 24 h in a Soxhlet apparatus to remove the impurities and oligomers. The insoluble fraction was then collected *via* extraction with CHCl$_3$ for 24 h. The chloroform solution is then concentrated to provide 0.34 g (71% yield) of orange precipitate. ^{1}H NMR (500 MHz, CDCl$_3$), (ppm, from TMS): 7.95–7.94(br, Ar–H), 7.63(br, Ar–H), 6.91(br, Ar–H and vinyl proton), 5.96(m, Ar–H), 4.11–3.49(m, –OCH$_2$– and –OCH$_3$), 1.94–1.25(m, –CH$_2$–), 1.01–0.86(m, –CH$_3$). (C$_{60}$H$_{78}$N$_4$O$_6$)$_n$ Elem. Anal. calcd: C, 75.75; H, 8.26; N, 5.89; Found: C, 75.66; H, 8.21; N, 5.80.

Polymer 8b (OXD-MEH-PPV(80/20)). The feed ratio between monomer **6** and monomer **7** is 80 : 20. The resulting copolymer was obtained as a brown powder with a yield of 65%. ^{1}H NMR (500 MHz, CDCl$_3$), (ppm, from TMS): 7.95–7.94(br, Ar–H), 7.63(br, Ar–H), 7.05–6.86(m, Ar–H and vinyl proton), 5.96(m, Ar–H), 4.12–3.79(m, –OCH$_2$– and –OCH$_3$), 0.97(m, –CH$_3$). [(C$_{60}$H$_{78}$N$_4$O$_6$)$_{0.80}$(C$_{17}$H$_{24}$O$_2$)$_{0.20}$]$_n$ Elem. Anal. calcd: C, 75.33; H, 8.37; N, 4.56; Found: C, 75.31; H, 8.41; N, 4.51.

Polymer 8c (OXD-MEH-PPV(67/33)). The feed ratio between monomer **6** and monomer **7** is 67 : 33. The resulting copolymer was obtained as a red powder with a yield of 54%. ^{1}H NMR (500 MHz, CDCl$_3$), (ppm, from TMS): 8.02–7.96(br, Ar–H), 7.66–7.63(br, Ar–H), 6.93–6.92(br, Ar–H and vinyl proton), 5.96(s, Ar–H), 4.13–3.92(m, –OCH$_2$– and –OCH$_3$), 2.96–1.25(m, –CH$_2$–), 1.02–0.87(m, –CH$_3$). [(C$_{60}$H$_{78}$N$_4$O$_6$)$_{0.67}$(C$_{17}$H$_{24}$O$_2$)$_{0.33}$]$_n$ Elem. Anal. calcd: C, 75.33; H, 8.37; N, 4.56; Found: C, 75.32; H, 8.39; N, 4.58.

Polymer 8d (OXD-MEH-PPV(50/50)). The feed ratio between monomer **6** and monomer **7** is 50 : 50. The resulting copolymer was obtained as a red powder with a yield of 51%. ^{1}H NMR (500 MHz, CDCl$_3$), (ppm, from TMS): 7.98–7.97(br, Ar–H), 7.64–7.62(br, Ar–H), 7.05–7.02(br, Ar–H and vinyl proton), 6.93–6.92(br, Ar–H), 4.14–3.94(m, –OCH$_2$– and –OCH$_3$), 1.95–1.25(m, –CH$_2$–), 1.01–0.87(m, –CH$_3$). [(C$_{60}$H$_{78}$N$_4$O$_6$)$_{0.50}$(C$_{17}$H$_{24}$O$_2$)$_{0.50}$]$_n$ Elem. Anal. calcd: C, 75.33; H, 8.37; N, 4.56; Found: C, 75.35; H, 8.37; N, 4.48.

Polymer 8e (OXD-MEH-PPV(33/67)). The feed ratio between monomer **6** and monomer **7** is 33 : 67. The resulting copolymer was obtained as a red powder with a yield of 52%. ^{1}H NMR (500 MHz, CDCl$_3$), (ppm, from TMS): 8.02–7.69(br, Ar–H),

7.47–7.44(br, Ar–H), 6.97–6.96(br, Ar–H and vinyl proton), 5.96(s, Ar–H), 4.15–3.94(m, –OCH$_2$– and –OCH$_3$), 1.95–1.23(m, –CH$_2$–), 1.01–0.87(m, –CH$_3$). [(C$_{60}$H$_{78}$N$_4$O$_6$)$_{0.33}$(C$_{17}$H$_{24}$O$_2$)$_{0.67}$]$_n$ Elem. Anal. calcd: C, 75.33; H, 8.37; N, 4.56; Found: C, 75.35; H, 8.31; N, 4.52.

Polymer 8f (OXD-MEH-PPV(20/80)). The feed ratio between monomer **6** and monomer **7** is 20 : 80. The resulting copolymer was obtained as a dark red powder with a yield of 53%. ^{1}H NMR (500 MHz, CDCl$_3$), (ppm, from TMS): 8.08–8.04(br, Ar–H), 7.54–7.49(br, Ar–H), 7.20–6.98(m, Ar–H and vinyl proton), 5.96(s, Ar–H), 4.17–3.94(m, –OCH$_2$– and –OCH$_3$), 1.83–1.25(m, –CH$_2$–), 1.01–0.88(m, –CH$_3$). [(C$_{60}$H$_{78}$N$_4$O$_6$)$_{0.20}$(C$_{17}$H$_{24}$O$_2$)$_{0.80}$]$_n$ Elem. Anal. calcd: C, 75.33; H, 8.37; N, 4.56; Found: C, 75.34; H, 8.32; N, 4.52.

Results and discussion

Synthesis and characterization

The synthetic routes for the 1,3,4-oxadiazole containing monomer **6**, corresponding polymers as well as copolymers with various ratios of OXD-PV and MEH-PV are shown in Scheme 1. Monomer **6** was synthesized in the following five steps. Diethyl 5-hydroxyisophthalate, **1**, was synthesized from 2,5-dimethylphenol by the reacting with 1,6-dibromo-hexane and potassium iodide in the presence of anhydrous potassium carbonate in acetone. Followed by the reaction in the mixture of 2,5-dimethyl-phenol, anhydrous potassium carbonate, potassium iodide and dry acetone, compound **2** was synthesized. After being treated with hydrazine monohydrate, the hydrazide, compound **3** was achieved. Condensation of hydrazide, **3**, with 4-dodecyloxy-benzoyl chloride yielded compound **4**, which is sufficiently pure for next step reaction. The result shows this method was feasible and the yield of compound **5** (56% for two steps) was considerable. After the bromination reaction with NBS, the newly designed monomer, **6** was obtained. The synthetic strategy of incorporating the oxadiazole-containing moiety as an ether linkage is trying to improve the solubility of the target polymer. In the co-monomer **7**, the bis(bromomethyl)-benzene backbone also contains two oxygen atom-linked side chains (a 2-ethyl-hexoxyl group and a methoxyl group) to provide a molecular similarity between the two monomers. In ^{1}H NMR spectra of monomer **6**, as shown in Fig. 1, benzyl

protons peaked at about 2.31 ppm and 2.18 ppm disappeared after bromination and two new peaks appeared at about 4.54 and 4.45 ppm, which confirmed the success of bromination. The purity of the monomers and the intermediate compounds were confirmed by ^{1}H NMR spectroscopy and elemental analysis.

Polymerization of monomer **6** was performed with an excess of potassium *tert*-butoxide in dry THF under nitrogen atmosphere at room temperature according to the standard Gilch method (Scheme 2). To tune the electro-optical properties of OXD-PPV, we copolymerized monomer **6**, with various feed ratios of monomer **7**, in THF. During the polymerization, the viscosity of the reaction mixture was increased without any precipitation, and intense fluorescent light was observed. In this work, the resulting polymers were completely soluble in common organic solvents, such as chloroform, tetrahydronfuran, and 1,1,2,2-tetrachloro-ethane. The good solubility of the OXD-MEH-PPVs is attributed to the easy free rotation between the PPV backbone and oxygen atom-linked bulky side chains.

Molecular weights and thermal properties

The molecular weights of the resulting copolymers are depicted in the Table 1. Using THF as the eluent and polystyrene as the standards, the GPC data exhibit a number-average (M_n) molecular weight from 8500 to 136 000 and a weight-average (M_w) molecular weight from 13 300 to 653 000, respectively. The polydispersity index (PDI) is from 1.55 to 4.86.

The thermal stability of polymer is important for device longevity. Fig. 2 displays the TGA chart of polymers **8a–8g**. The TGA analysis reveals that, a relatively high thermal stability with an initial weight loss (5%) temperature of 312 °C, extending to 326 °C. It is interesting to observe that the thermal stabilities of the polymers are progressively improved with the increasing amount of oxadiazole-containing moieties.

Optical properties

1. Ultraviolet-visible (UV-vis) spectroscopies of polymers 8a–8g. The UV-vis absorption properties of polymers **8a–8g**
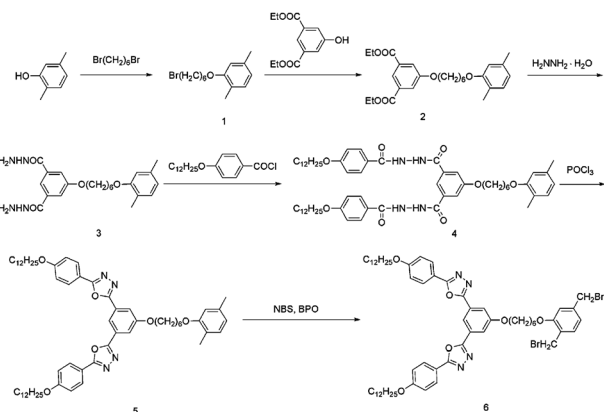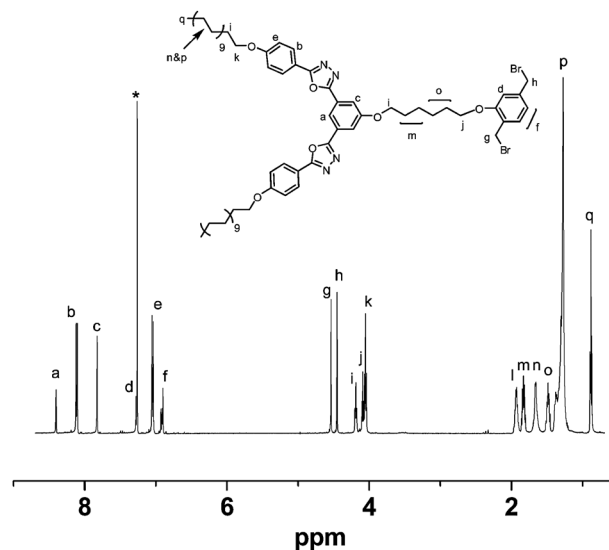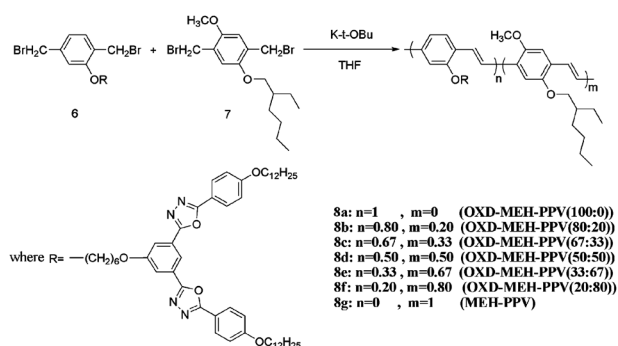

Scheme 1 Synthesis of monomer **6**.

Fig. 1 ^{1}H NMR spectrum and chemical structure of the monomer **6** in CDCl$_3$ solution.

8a: n=1 , m=0 (OXD-MEH-PPV(100:0))
8b: n=0.80, m=0.20 (OXD-MEH-PPV(80:20))
8c: n=0.67, m=0.33 (OXD-MEH-PPV(67:33))
8d: n=0.50, m=0.50 (OXD-MEH-PPV(50:50))
8e: n=0.33, m=0.67 (OXD-MEH-PPV(33:67))
8f: n=0.20, m=0.80 (OXD-MEH-PPV(20:80))
8g: n=0 , m=1 (MEH-PPV)

where R= —$(CH_2)_8$O—

Scheme 2 Synthesis of copolymers.

Table 1 Polymerization results and thermal properties of polymers **8a–8g**

Polymer	Feed ratio	M_n^a (10⁴)	M_w^a (10⁴)	PDI	T_d^b (°C)
8a (100/0)	100 : 0	13.6	60.1	4.41	326
8b (80/20)	80 : 20	0.85	1.33	1.55	319
8c (67/33)	67 : 33	2.39	10.6	4.44	318
8d (50/50)	50 : 50	12.6	61.4	4.86	317
8e (33/67)	33 : 67	12.5	37.4	2.99	315
8f (20/80)	20 : 80	7.5	12.3	1.63	312
8g (0/100)	0 : 100	19.7	65.3	3.30	303

^{a} Calculated from GPC (eluent : THF; polystyrene standards). ^{b} Temperature at 5% weight loss by a heating rate of 10 °C min⁻¹ under nitrogen.

are presented in Table 2. Fig. 3 shows the normalized UV-vis absorption of the copolymers in CHCl₃ solution and film spin-coated from CHCl₃ solution.

The absorption spectra of polymers **8a–8f** in the solutions of CHCl₃ display two absorption bands. The long wavelength peak in the region of 400–550 nm originates from the π–π* absorption of the conjugated polymer main chain, whereas the short wavelength peak around 304 nm is attributed to the aromatic side chain.[12,32] It is interesting to observe that, with the increasing amount of 1,3,4-oxadiazole moieties, the intensity of the absorption at 453–486 nm decreased gradually while that at around 304 nm increased gradually. Compared with the absorption peak of MEH-PPV at 499 nm, the polymers exhibit blue-shifted peaks, and the degree of the blue-shift increases with the increasing amount of 1,3,4-oxadiazole moieties. We believe the blue-shift arises from the reduced
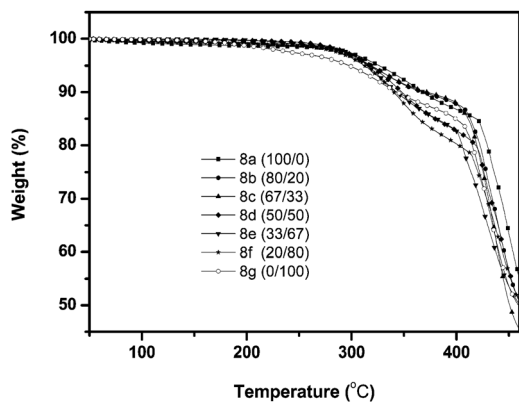

Fig. 2 TGA thermogram of polymers **8a–8g**.

Table 2 Optical data of polymers **8a–8g**

Polymer	In solution^a		In film^b		Optical^c	
	λ_{max}^{abs}/nm	λ_{max}^{em}/nm	λ_{max}^{abs}/nm	λ_{max}^{em}/nm	E_g^{opt}/eV	Φ_{PL}
8a (100/0)	453/305	516	452/313	535	2.31	0.26
8b (80/20)	463/304	522	468/306	548	2.28	0.18
8c (67/33)	470/305	532	489/309	564	2.21	0.21
8d (50/50)	478/403	538	489/303	564	2.19	0.21
8e (33/67)	479/304	547	497/315	573	2.17	0.22
8f (20/80)	486/304	550	505/314	574	2.16	0.12
8g (0/100)	499/332	554	510	585	2.12	0.10

^{a} 1 × 10⁻⁵ M in anhydrous chloroform. ^{b} Spin-coated from a 5 mg mL⁻¹ chloroform solution. ^{c} The optical band gap (E_g^{opt}) was obtained from absorption edge.
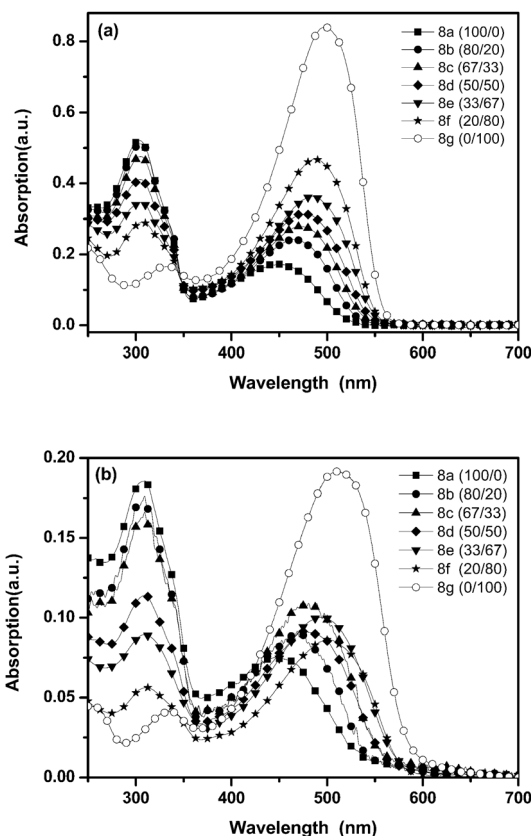
Fig. 3 UV-vis absorption spectra of polymers **8a–8g** in (a) CHCl₃ solution and (b) films.

content of electron-donating oxygen atom attached to the phenylene ring in the main chain and also due to the reduced coplanarity of the polymer main chain.[23,24] The bulky substituent in polymers **8a–8f** causes the steric hindrance and will make the phenylene ring or vinylene unit twist; therefore, the π-conjugation will be interrupted.[24] The absorbance spectra of the copolymers in solid thin films are similar to those of the copolymers in CHCl₃ solutions, except for the red-shift of the longer wavelength peaks, which suggests more efficient π-stacking and stronger intermolecular interactions in the film.[12] The distinguishable absorption features of polymers **8a–8g** demonstrate that OXD-PV unit was successfully incorporated into the PPV-based polymer backbone with a pre-defined feed ratio.

2. Photoluminescent (PL) spectroscopies of polymers 8a–8g.
Fig. 4 outlines the photoluminescence spectra of polymers **8a–8g** in both CHCl$_3$ solution and film spin-coated from CHCl$_3$ solution. The characteristic values are listed in Table 2.

The emission spectra are quite similar for the solution and film samples with one main emission peak. Interestingly, as OXD-PV content is increased, the wavelength of the maximum emission peak of polymers **8a–8f** exhibits a gradually blue-shifted trend in both solution and film, which is attributed to the reduced amount of electron-donating oxygen atom attached to the backbone and the increased amount of bulky substituents.[23,24]

In Table 2, we listed the PL quantum efficiencies (Φ_{PL}) of the solid film of the polymers, which were measured under a 405 nm Ocean Optics LLS-LED in the integrating sphere. The PL quantum efficiencies of the OXD-MEH-PPVs range from 12% to 26%, which are higher than that of MEH-PPV (10%), indicating that the OXD-PV unit can greatly enhance the absolute PL quantum efficiencies of the copolymers. With the OXD-PV content of 100%, the highest Φ_{PL} value of 26% is achieved for polymer **8a** (OXD-PPV). With the incorporation of an OXD-PV moiety, the PL quantum efficiencies of the polymers were increased, indicating that the long, flexible side chains can dilute the main chains like a solvent, causing a reduction in the aggregation of conjugational segments, and thus an increase in PL quantum efficiency.[14,33]

Electrochemical properties

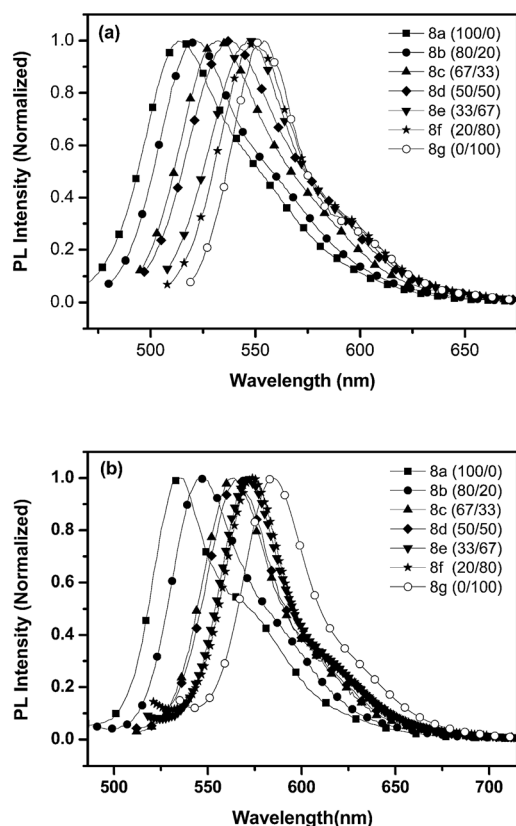Cyclic voltammogram (CV) is very helpful in measuring electrochemical behaviors and evaluating the relative HOMO, LUMO energy levels and the band gap of a polymer.[34] Fig. 5 shows the cyclic voltammograms of the polymers **8a–8g**, which were performed at room temperature in anhydrous acetonitrile, using a platinum disk as the working electrode, a platinum wire as the counter electrode, an Ag/AgNO$_3$ as the reference electrode, and tetrabutylammonium hexafluorophosphate (TBAPF$_6$, 0.1 mol L^{-1}) as the supporting electrolyte. Ferrocene/ ferrocenim (Fc/Fc$^+$) was used as the internal reference and showed a peak at +0.05 V vs. Ag/Ag$^+$.

From the onset oxidation potentials (E_{ox}^{onset}) and the onset reduction potentials (E_{red}^{onset}) of the polymers, HOMO and LUMO energy levels as well as the energy gap were calculated according to the following equations:[35–38]

$$\text{HOMO (eV)} = -e(E_{ox}^{onset} + 4.75)$$

$$\text{LUMO (eV)} = -e(E_{red}^{onset} + 4.75)$$

$$E_g^{ec}\ (\text{eV}) = e(E_{ox}^{onset} - E_{red}^{onset})$$

where E_{ox}^{onset} and E_{red}^{onset} are the measured potentials relative to Ag/Ag$^+$.

The electrochemical properties of the copolymers are listed in Table 3 and their band diagram is shown in Fig. 6. Obviously, as the 1,3,4-oxadiazole units in the polymers increased, their HOMO energy levels gradually decreased. Similarly, their LUMO energy levels showed a decreasing tendency after introducing more electron-withdrawing pendant groups. Regarding that the threshold HOMO level for air stable conjugated polymers is estimated to be −5.2 eV,[39] it is concluded that attaching 1,3,4-oxadiazole units to polymers can effectively lower their HOMO levels, thus enhancing their chemical stability in ambient conditions. The optical band gaps estimated from absorption onset of the copolymers are significantly less than the electrochemical data.

Mobility

To investigate the influence of Y-shaped side chain on the PPVs' charge-transport abilities, we estimated the hole mobility and electron mobility of polymer **8a** (OXD-MEH-PPV (100 : 0)) by the space-charge-limited-current (SCLC) method.[40–42] The J–V curves of the ITO/polymer **8a**/LiF/Al device and the
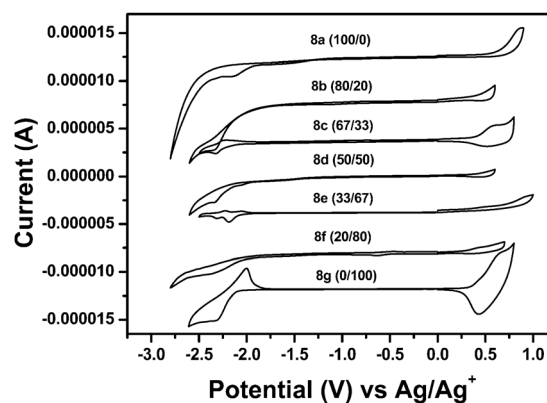

Fig. 4 Normalized photoluminescence spectra of polymers **8a–8g** in (a) CHCl$_3$ solution and (b) films.

Fig. 5 Cyclic voltammograms of the films of polymers **8a–8g** cast on a platinum electrode in 0.1 M TBAPF$_6$ in acetonitrile at a 50 mV s^{-1} scan rate.

Table 3 Electrochemical data of polymers **8a–8g**

Polymer	E_{ox}^{onset}/eV	E_{red}^{onset}/eV	HOMO/eV	LUMO/eV	E_g^{ec}/eV
8a (100/0)	0.65	−1.97	−5.40	−2.78	2.62
8b (80/20)	0.44	−2.05	−5.19	−2.70	2.49
8c (67/33)	0.41	−2.07	−5.16	−2.68	2.48
8d (50/50)	0.40	−2.07	−5.16	−2.68	2.47
8e (33/67)	0.39	−2.08	−5.14	−2.67	2.47
8f (20/80)	0.37	−2.06	−5.12	−2.69	2.43
8g (0/100)	0.36	−2.10	−5.11	−2.65	2.46
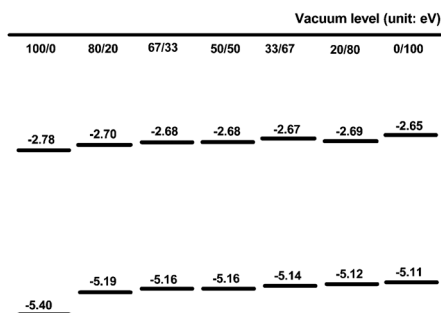
Fig. 6 Band diagram of polymers **8a–8g**.

ITO/PEDOT:PSS/polymer **8a**/Au device in the dark are shown in the Supplementary Information.†

The electron mobility and the hole mobility of polymer **8a** are estimated according to the following equation

$$J = \frac{9}{8}\varepsilon_r\varepsilon_0\mu\frac{(V - V_{bi})^2}{L^3}$$

where V is the applied voltage, J is the current density, ε_r and ε_0 are the relative dielectric constant and permittivity of free space (8.85×10^{-12} F m^{-1}), respectively, μ represents μ_e (the electron mobility) or μ_h (the hole mobility). L is the thickness of the corresponding organic layer, and ε_r is fitted as 3.0. As for the electron mobility, we fit V_{bi} as 0.7 V; as for the hole mobility, we fit V_{bi} as 0.2 V.

The electron mobility of polymer **8a** is estimated to be 2.77×10^{-5} cm^2 V^{-1} s^{-1}, which is 3 orders of magnitude higher than that of MEH-PPV ($\sim 10^{-8}$ cm^2 V^{-1} s^{-1}).[43,44] The hole mobility of polymer **8a** is estimated to be 7.44×10^{-8} cm^2 V^{-1} s^{-1}, which is very close to that of MEH-PPV ($\sim 10^{-7}$ cm^2 V^{-1} s^{-1}).[45,46] With the introduction of a Y-shaped side chain, the electron mobility of polymer **8a** is significantly enhanced, while the main chain PPV does retain its own hole mobility, indicating that the double 1,3,4-oxadiazole-containing side chain is very effective in improving the PPVs' electron-transporting ability.

Conclusions

We have designed and synthesized a series of novel PPV-based polymers OXD-MEH-PPVs *via* modified Gilch reaction. All the polymers exhibit high molecular weights and good solubility in common organic solvents. They also show improved thermal stability by incorporating more oxadiazole-containing moieties. Optical property investigations of the polymers indicate that the absorption and emission bands were blue-shifted by incorporating more oxadiazole-containing moieties. With the incorporation of

OXD-PV units, OXD-MEH-PPVs also exhibit enhanced PL quantum efficiencies, compared with that of MEH-PPV. Moreover, as demonstrated from the investigation of electrochemical properties, the HOMO and LUMO levels of the polymers exhibit a decreasing tendency after incorporating more oxadiazole-containing moieties. These results prove that the design of a Y-shaped, double 1,3,4-oxadiazole-containing, bulky side chain is very successful in tailoring the photophysical and electrochemical properties of PPV-based polymers, which provides a better understanding on how the chemical structures affect polymer's optical and electronic properties. High molecular weights along with good thermal stability, good air-stability, adjustable spectral properties and energy levels indicate that OXD-MEH-PPVs are promising materials for optoelectronic applications.

Notes and references

1 G. Gustafsson, Y. Cao, G. M. Treacy, F. Klavetter, N. Colaneri and A. J. Heeger, *Nature*, 1992, **357**, 477.
2 R. H. Friend, R. W. Gymer, A. B. Holmes, J. H. Burroughes, R. N. Marks, C. Taliani, D. D. C. Bradley, D. A. Dos Santos, J. L. Bredas, M. Logdlund and W. R. Salaneck, *Nature*, 1999, **397**, 121.
3 N. Blouim, A. Michaud and M. Leclerc, *Adv. Mater.*, 2007, **19**, 2295.
4 C. J. Brabec, N. S. Sariciftci and J. C. Hummelen, *Adv. Funct. Mater.*, 2001, **11**, 15.
5 F. Huang, Y. Zhang, M. S. Liu, Y.-J. Cheng and A. K.-Y. Jen, *Adv. Funct. Mater.*, 2007, **17**, 3808.
6 N. Blouim, A. Michaud, D. Gendron, S. Wakim, E. Blair, R. Neagu-Plesu, G. Durocher, Y. Tao and M. Leclerc, *J. Am. Chem. Soc.*, 2008, **130**, 732.
7 J. Li, F. Dierschke, J. S. Wu, A. C. Grimsdale and K. Müllen, *J. Mater. Chem.*, 2006, **16**, 96.
8 P. D. Vellis, J. A. Mikroyannidis, M. J. Cho and D. H. Choi, *J. Polym. Sci., Part A: Polym. Chem.*, 2008, **46**, 5592.
9 P. Wang, C. H. Chai, Q. Yang, F. Z. Wang, Z. H. Shen, H. Q. Guo, X. F. Chen, X. H. Fan, D. C. Zou and Q. F. Zhou, *J. Polym. Sci., Part A: Polym. Chem.*, 2008, **46**, 5452.
10 K.-M. Yeh, C.-C. Lee and Y. Chen, *J. Polym. Sci., Part A: Polym. Chem.*, 2008, **46**, 5180.
11 J. H. Hou, L. J. Huo, C. He, C. H. Yang and Y. F. Li, *Macromolecules*, 2006, **39**, 594.
12 S. P. Wen, J. N. Pei, Y. H. Zhou, L. L. Xue, B. Xu, Y. W. Li and W. J. Tian, *J. Polym. Sci., Part A: Polym. Chem.*, 2009, **47**, 1003.
13 W. P. Su, K. M. Yen and Y. Chen, *J. Polym. Sci., Part A: Polym. Chem.*, 2007, **45**, 4377.
14 L. S. Yu and S. A. Chen, *Adv. Mater.*, 2004, **16**, 744.
15 S. D. Xun, Q. G. Zhou, H. C. Li, D. G. Ma, L. X. Wang, X. B. Jing and F. S. Wang, *J. Polym. Sci., Part A: Polym. Chem.*, 2008, **46**, 1566.
16 C.-H. Kuo, W.-K. Cheng, K.-R. Lin, M.-K. Leung and K.-H. Hsieh, *J. Polym. Sci., Part A: Polym. Chem.*, 2007, **45**, 4504.
17 H.-J. Cho, D.-H. Hwang, J.-D. Lee, N.-S. Cho, S.-K. Lee, J. Lee, Y. K. Jung and H.-K. Shim, *J. Polym. Sci., Part A: Polym. Chem.*, 2008, **46**, 979.
18 P. Kratatiris, J. A. Mikroyannidis and I. K. Spiliopoulos, *J. Polym. Sci., Part A: Polym. Chem.*, 2008, **46**, 2367.
19 M. M. Wienk, J. M. Kroon, W. J. H. Verhees, J. Knol, J. C. Hummelen, P. A. Hal and R. A. J. Janssen, *Angew. Chem., Int. Ed.*, 2003, **42**, 3371.

20 K. Ajima, Y. Suzuki and K. Hasshimoto, *J. Phys. Chem. C*, 2008, **112**, 8507.

21 R. P. Tang, Z. A. Tan, C. X. Cheng, Y. F. Li and F. Xi, *Polymer*, 2005, **46**, 5341.

22 S. H. Jin, M. Y. Kim, J. Y. Kim, K. Lee and Y. S. Gal, *J. Am. Chem. Soc.*, 2004, **126**, 2474.

23 Y.-Z. Lee, X. Chen, S.-A. Chen, P.-K. Wei and W.-S. Fann, *J. Am. Chem. Soc.*, 2001, **123**, 2296.

24 Z.-K. Chen, H. Meng, Y.-H. Lai and W. Huang, *Macromolecules*, 1999, **32**, 4351.

25 K. Lee, H.-J. Kim, J. C. Cho and J. Kim, *Macromolecules*, 2007, **40**, 6457.

26 W.-L. Yu, H. Meng, J. Pei, W. Huang, Y. Li and A. J. Heeger, *Macromolecules*, 1998, **31**, 4838.

27 W.-L. Yu, H. Meng, J. Pei and W. Huang, *J. Am. Chem. Soc.*, 1998, **120**, 11808.

28 W.-L. Yu, H. Meng, J. Pei, Y.-H. Lai, S.-J. Chua and W. Huang, *Chem. Commun.*, 1998, 1957.

29 W. Huang, H. Meng, W.-L. Yu, J. Pei, Z.-K. Chen and Y.-H. Lai, *Macromolecules*, 1999, **32**, 118.

30 S. R. Amrutha and M. Jayakannan, *J. Phys. Chem. B*, 2006, **110**, 4083.

31 C. J. Neef and J. P. Ferraris, *Macromolecules*, 2000, **33**, 2311.

32 H. Meng, W. L. Yu and W. Huang, *Macromolecules*, 1999, **32**, 8841.

33 L. J. Huo, J. H. Hou, Y. Zhou, M. F. Han and Y. F. Li, *J. Appl. Polym. Sci.*, 2008, **110**, 1002.

34 Y. W. Li, L. L. Xue, H. J. Xia, B. Xu, S. P. Wen and W. J. Tian, *J. Polym. Sci., Part A: Polym. Chem.*, 2008, **46**, 3970.

35 Z. G. Zhang, Y. L. Liu, Y. Yang, K. Y. Hou, B. Peng, G. J. Zhao, M. J. Zhang, X. K. Guo and Y. F. Li, *Macromolecules*, 2010, **43**, 9376.

36 S. P. Wen, Q. F. Dong, W. D. Cheng, P. F. Li, B. Xu and W. J. Tian, *Sol. Energy Mater. Sol. Cells*, 2012, **100**, 239.

37 S. P. Wen, J. N. Pei, P. F. Li, Y. H. Zhou, W. D. Cheng, Q. F. Dong, Z. F. Li and W. J. Tian, *J. Polym. Sci., Part A: Polym. Chem.*, 2011, **49**, 2715.

38 S. P. Wen, J. N. Pei, Y. H. Zhou, P. F. Li, L. L. Xue, Y. W. Li, B. Xu and W. J. Tian, *Macromolecules*, 2009, **42**, 4977.

39 Z. F. Li, J. N. Pei, Y. W. Li, B. Xu, M. Deng, Z. Y. Liu, H. Li, H. G. Lu, Q. Li and W. J. Tian, *J. Phys. Chem. C*, 2010, **114**, 18270.

40 Y. H. Zhou, J. N. Pei, Q. F. Dong, X. B. Sun, Y. Q. Liu and W. J. Tian, *J. Phys. Chem. C*, 2009, **113**, 7882.

41 J. N. Pei, S. P. Wen, Y. H. Zhou, Q. F. Dong, Y. Q. Liu, J. B. Zhang and W. J. Tian, *New J. Chem.*, 2011, **35**, 385.

42 P. W. M. Blom, M. J. M. deJong and M. G. vanMunster, *Phys. Rev. B*, 1997, **55**, R656.

43 H. S. Kang, K. H. Kim, M. S. Kim, K. T. Park, K. M. Kim, T. H. Lee, J. Joo, K. Kim, D. W. Lee and J. I. Jin, *Curr. Appl. Phys.*, 2001, **1**, 443.

44 H. S. Kang, K. H. Kim, M. S. Kim, K. T. Park, K. M. Kim, T. H. Lee, C. Y. Lee, J. Joo, D. W. Lee, Y. R. Hong, K. Kim, G. J. Lee and J. I. Jin, *Synth. Met.*, 2002, **130**, 279.

45 A. J. Breeze, Z. Schlesinger and S. A. Carter, *Phys. Rev. B*, 2001, **64**, 125205.

46 G. G. Malliaras, J. R. Salem, P. J. Brock and C. Scott, *Phys. Rev. B*, 1998, **58**, R13411.